



RESPONSE OF NON-AXISYMMETRICAL FOUNDATIONS SUBJECTED TO DYNAMIC EXCITATION

M. SUAREZ and F.J. SÁNCHEZ-SESMA

Instituto de Ingeniería,
Universidad Nacional Autónoma de México, México

ABSTRACT

The influence in dynamic response of foundation shape in the soil-structure interaction problem is studied. The structure is assumed to be founded in a homogeneous, viscoelastic layer which rests on a rigid moving base or in a half-space where an elastic wave field impinge with different angles. Impedance functions and driving forces are obtained for various three-dimensional configurations. Computations are performed using the indirect boundary element method (IBEM) where the diffracted waves are constructed from the radiation of sources located at the boundaries. The analysis is made in the frequency domain. The results of a parametric study are presented.

KEYWORDS

Impedance functions, driving forces, foundation input motion.

INTRODUCTION

In soil-structure interaction one of the factors that affects the response of the foundation when is subjected to a dynamic excitation is its shape. Dobry and Gazetas (1986) concluded that the foundation shape may significantly affect both dynamic stiffnesses and dampings. Additional torsion and rocking effects can appear in structures with irregular foundation shape. The embedment also contributes to modify the dynamic response.

An important issue to consider is the thickness and mechanical properties of the layered medium where the structure is founded. In a stratified medium, the dynamic response differs from that obtained for a structure on a half-space basically because a significant part of the vibrational energy is trapped in the system and only the soil surrounding the foundation contributes to dissipate it by hysteresis or other mechanisms. On the other hand, in the half-space, in addition to the material damping, an important amount of energy is radiated away. All this affects the frequency and the amplitude of peak response.

In this paper, the indirect boundary element method (IBEM) is applied to compute the seismic response of

arbitrarily shaped, yet not very elongated, three-dimensional foundations. Special attention is given to the embedment of the foundation and the angle of incidence of the wavefield. The results are plotted in terms of the normalized frequency η ($\eta=\omega a/\pi\beta$, where ω =circular frequency, a =reference length and β =shear wave velocity).

MODEL STUDIED

Fig. 1 depicts the model under scrutiny. The foundation is assumed to be rigid and perfectly bonded to an elastic and homogeneous soil medium. Two problems are studied: the foundation is a) resting in a half-space and b) resting in a layer of thickness H with a moving rigid base. In the analysis we obtain the radiated (or the scattered) displacement field associated to the presence of the foundation ($u^{(s)}$). At a point x , $u^{(s)}$ can be represented by a single layer boundary integral as

$$u_i^{(s)}(x) = \int_S \phi_j(\xi) G_{ij}(x, \xi) dS_\xi \quad (1)$$

where $u_i^{(s)}(x)$ = i th component of displacement at x , $G_{ij}(x, \xi)$ =Green's function i.e. the displacement in direction i at x due to a unit force applied at point ξ with direction j , and ϕ_j =force density in direction j . $\phi_j(\xi)dS_\xi$ is the force distribution at the surface S along where the integration is made (Sánchez-Sesma and Campillo, 1991).

The integral representation of eq. (1) allows the computation of the tractions $t_i^{(t)}$ in point x by the following expression

$$t_i^{(t)}(x) = t_i^{(0)}(x) + c\phi_i(x) + \int_S \phi_j(\xi) T_{ij}(x, \xi) dS_\xi \quad (2)$$

where $t_i^{(t)}$ = i th component of traction at the smooth boundary of the layer. The superscripts t and 0 refer to the total and the free fields, respectively. The free field is the response to a dynamic excitation before any excavation for the foundation is made. $c=0.5$ or $c=0$ if x at S (which is assumed to be smooth) or if x is not at S , respectively. $T_{ij}(x, \xi)$ = traction Green's function at x in the direction i on the boundary, with normal $n(x)$, due to a unit force with direction j at point ξ . Subscripts in the differential indicate the space variable over which the integration is performed. The exact Green's function in unbounded elastic space can be found in Sánchez-Sesma and Luzón (1995).

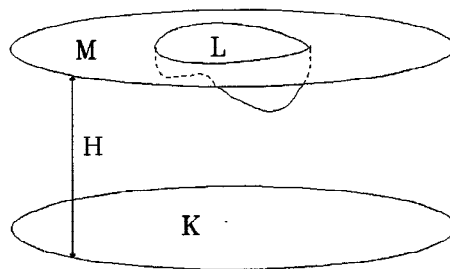


Fig. 1. Non-axisymmetric 3D foundation L . K is the rigid base, M the free surface and H is the layer's thickness.

The surface S is divided in three regions called K , L and M which correspond to the boundaries between the layer and the rigid base, the layer and the foundation and the free surface, respectively (Fig. 1). The boundary conditions for the computation of the driving forces consider the total field of tractions ($t^{(t)}$) and displacement ($u^{(t)}$). The tractions are null ($t^{(t)}(x)=0$) in region M , there are no displacements ($u^{(t)}(x)=0$) in

L and $u^{(0)}(x)=u^{(0)}(H)$ in K . On the other hand, for the impedance functions the boundary conditions are $u^{(0)}(x)=0$ in M , $u^{(0)}(x)=1$ in L and $u^{(0)}(x)=0$ in K . $u^{(0)}=u^{(0)}+u^{(s)}$, $u^{(0)}$ is the displacement of the free-field, its calculation is performed using standard methods of the elastic wave propagation theory (e.g. Aki and Richards, 1980). Eqs. (1) and (2) are discretized along S in N boundary small surfaces with dimensions that depend on the analysed frequency. This leads to a system of $3N$ linear equations from which $\phi_j(\xi)$ are obtained. Then, the driving forces along the region L and the forces and moments generated by the motion (displacements and rotations) of the rigid foundation can be obtained. The accuracy of this method has been verified through the comparison of results with those obtained by other methods (see Suarez and Sánchez-Sesma, 1995).

In what follows the response of foundation shapes shown in Fig. 2 when are subjected to a dynamic excitation are discussed. All the computations are made considering a material damping and Poisson's ratio of 0.05 and 1/3, respectively.

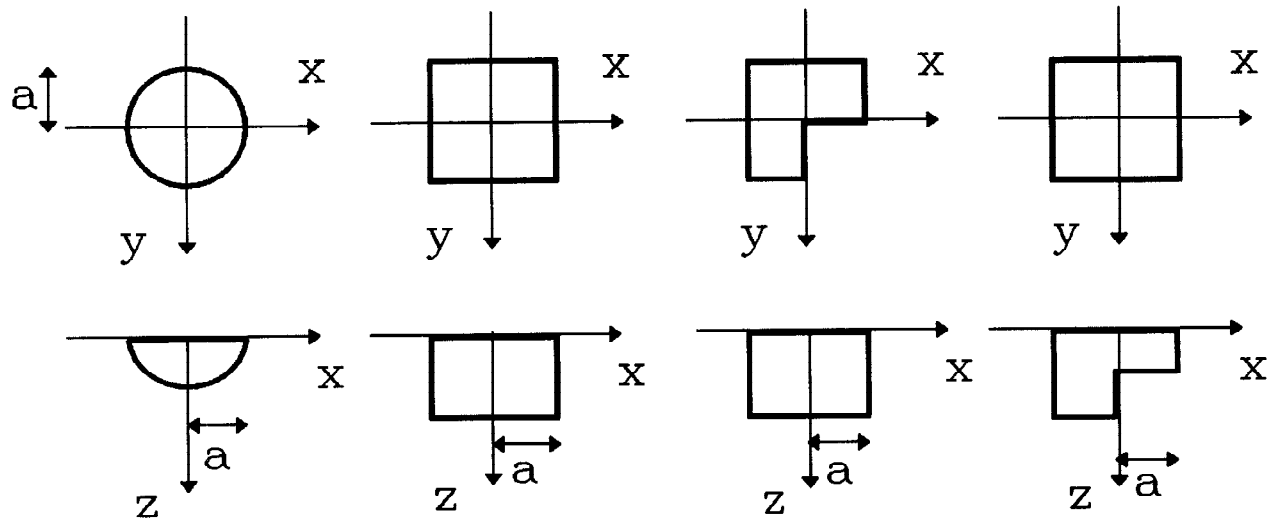


Fig. 2. Foundation shapes studied. In this text they are called *hemisphere*, *square*, *LPL* ('L' shape in a x-y coordinate system) and *LEL* ('L' shape in a x-z coordinates), respectively.

IMPEDANCE FUNCTIONS

The impedance functions (K_{ij}) are the forces (or moments) in direction j applied in the foundation when it is moved with an unitary displacement (or rotation) in direction i . They can be expressed in the form $K=K_0(k+ic\eta)$ (see Lee, 1979), where K_0 is the static stiffness. The amplitudes of the plotted curves correspond to the ratio between the functions obtained and their value at static stage (that is k and c). In Fig. 3 the horizontal, rocking, torsional and coupling impedance functions are depicted for the foundation shapes presented in Fig. 2 with an embedment a in a half-space (a is the lateral half-width of the foundation). In general, it can be seen that the stiffnesses decrease for high frequencies while damping curves tend to increase for the frequencies studied. The main differences observed for the foundation shapes analyzed are in horizontal and torsion impedances. These differences are more pronounced for the *hemisphere* specially for high frequencies. For *square*, *LPL* and *LEL* foundations the responses obtained are very similar, except for the horizontal dampings where there is a reduction of their amplitude for non-axisymmetric foundations that are less efficient to radiate the energy; probably because it is trapped in the soil which is located in the entrances of foundation shapes.

Figs. 4 and 5 show the impedances for a *LPL* foundation. In Fig. 4 the results were obtained considering different embedments (h) in a half-space. The horizontal impedances are significantly affected by the embedment of the foundation. Rocking and torsion stiffnesses are very similar while dampings vary in an important way for high frequencies. In horizontal damping this variations are for all frequencies. Horizontal stiffness has also important differences. From these plots it is clear that deeper foundations are more efficient to radiate energy. In Fig. 5 the impedances for an embedment a in a layer of thicknesses H are presented. As expected, for thick layers the results obtained for this foundation shape get closer to the behaviour of the curves computed for the half-space. In layers of moderated thicknesses the amplitudes oscillate with great peaks. This is because of the energy that is trapped in a layer. In a half-space, this energy is radiated.

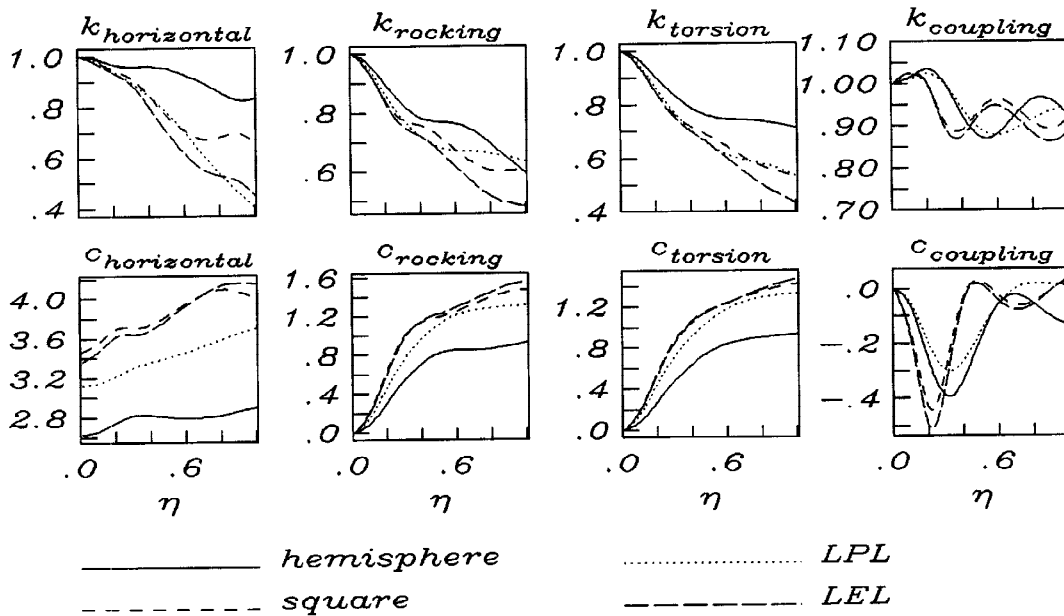


Fig. 3. Impedance functions for different foundation shapes (see Fig. 2) with an embedment a

DRIVING FORCES

The driving forces are computed by integration of the tractions $t_j(\xi)$ along the region L. In Figs. 6, 7 and 8 the foundation input motions are plotted. They are computed multiplying the flexibility matrix (K_{ij}^{-1}) by the driving forces (Kausel *et al.*, 1978). The amplitudes obtained were normalized with respect to the incident field. The embedment considered for the foundations was a . Fig. 6 shows the curves plotted for different foundation shapes when are subjected to incoming *SH* waves with an incident angle of 30° . Again, the influence of the foundation's geometry is significant for hemispherical foundations, being more important for rocking and torsion. In Fig. 7 the normalized displacements amplitudes of a *LPL* foundation under the incidence of *P* waves are shown for different angles. The angle of incidence is one of the factors with more influence in the variation of the dynamic response of the foundation. For foundations in a layer with thickness H the results are strongly affected by its resonant frequency. Considering that the resonant non-dimensional frequency for a layer can be computed by $\eta_n = (2n+1)a/(2H)$, the large amplifications observed in results obtained for a *LPL* foundation subjected to an incident angle of 30° of *SH* waves (Fig. 8) can be explained in these terms.

Figs. 9 and 10 show the soil structure interaction response obtained when the system is excited by a field of *SH* waves that incide with an angle of 30° with an embedment a . For the computations we considered a foundation with mass ratio density $\rho_F/\rho_s=1$ (ρ_F =foundation and ρ_s =soil mass density). In Fig. 9 the

displacements (Δ) and rotations (ϕ) are plotted for the foundation shapes shown in Fig. 2. Displacements in horizontal direction are similar for all the foundation shapes studied, whereas for torsion and rocking the differences become important for high frequencies. Fig. 10 shows the dynamic response for the soil-foundation-single degree of freedom oscillator. In this figure square foundations were studied. The mass density ratio of the oscillator (ρ_b) over the soil mass density (m_s) is varied to analyze its influence in the response. The results computed show that the horizontal displacement is almost the same for any mass ratio and torsion is not affected. On the other hand, rocking presents important differences in high frequencies for *LPL* and *LEL* in comparison with *hemispherical* and *square* foundations.

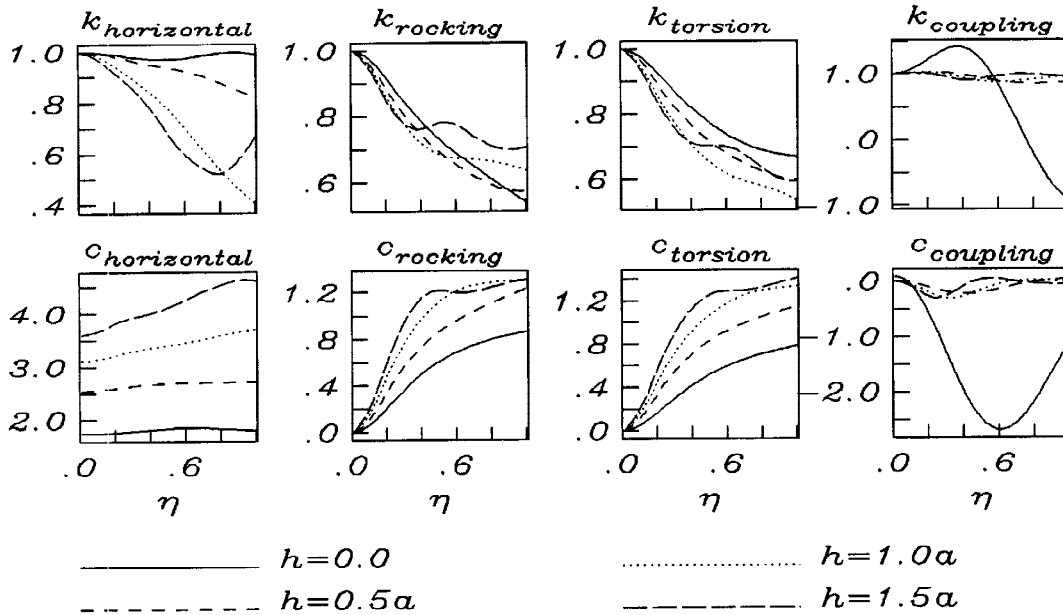


Fig. 4 Impedances functions for a *LPL* foundation with an embedment h in a half-space.

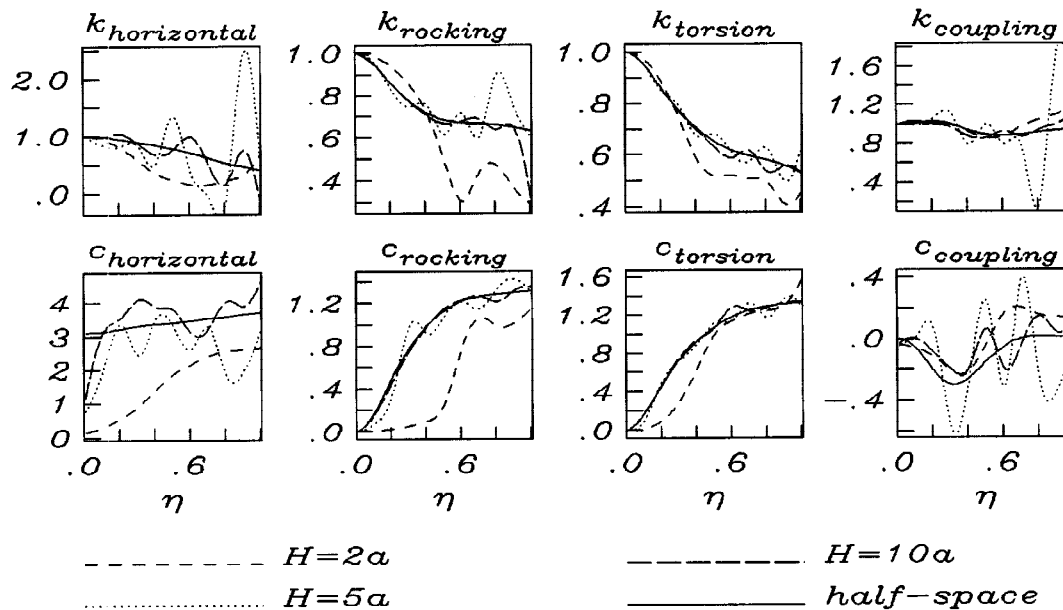


Fig. 5 Impedances functions for a *LPL* foundation with an embedment a in a layer with a thickness H .

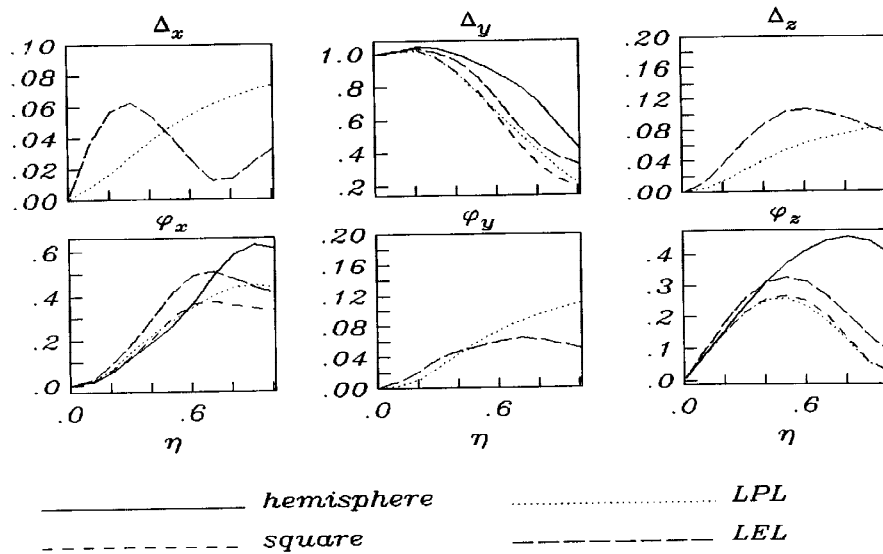


Fig. 6 Foundation input motion for different foundation shapes (see Fig. 2) with an embedment a subjected to SH waves with an incidence of 30° .

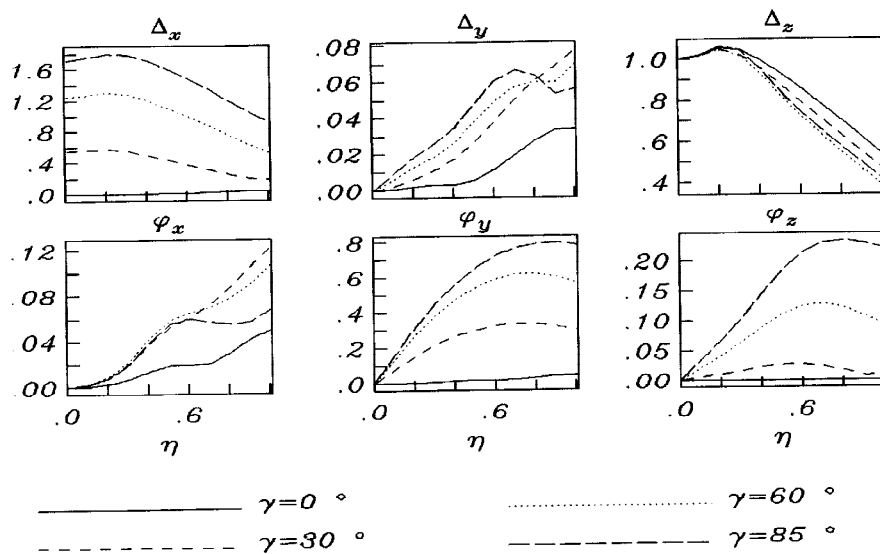


Fig. 7 Foundation input motion for a LPL foundation with an embedment a in a half-space subjected to P waves with an incidence γ .

CONCLUSIONS

The IBEM was applied to compute the impedance functions and driving forces for foundations on an elastic layer or on a half-space. We found significant effects associated to foundation shape, incident angle and layer's thickness. In computations of the impedance functions, the influence of geometry in the damping of energy can be very important, while the stiffnesses variation is moderate, except for the horizontal stiffness. Both, driving forces and impedancies behavior is strongly affected when considering a foundation embedded in a layer. Foundation input motion is governed by the natural frequency of the layer.

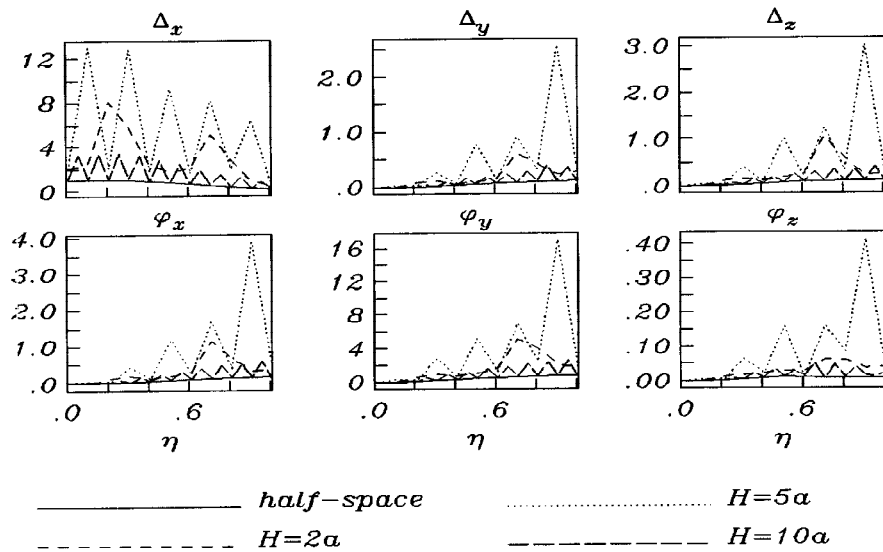


Fig. 8 Impedances functions for a LPL foundation with an embedment a in a layer with a thickness H .

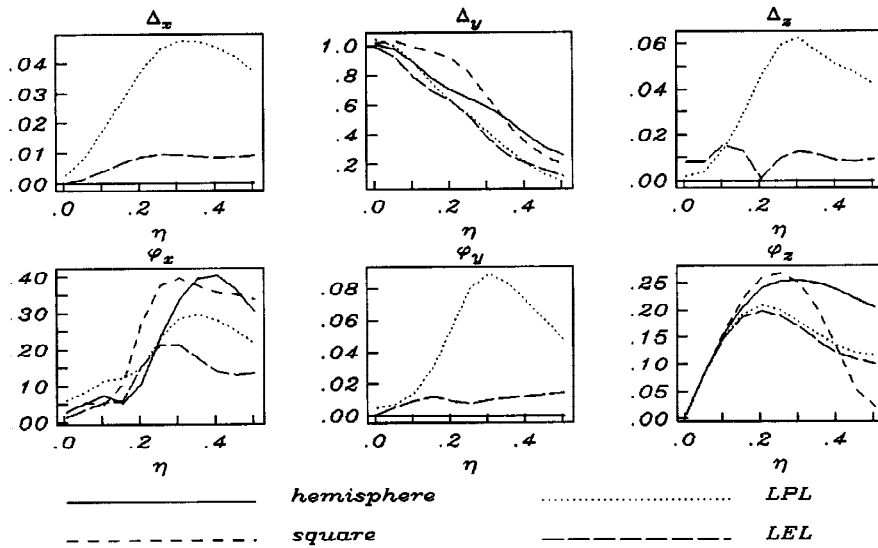


Fig. 9 Foundation input motion for different foundation shapes (see Fig. 2) with an embedment a subjected to SH waves with an incidence of 30° .

ACKNOWLEDGMENTS

Figs. 9 and 10 were computed with a program kindly provided by M. Todorovska. This work was partially supported by Secretaría General de Obras del Departamento del Distrito Federal, México.

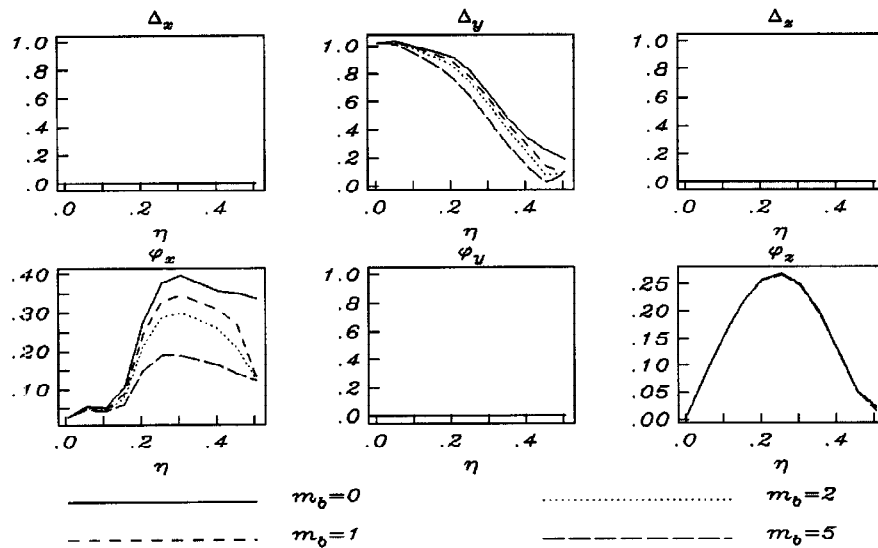


Fig. 10 Foundation input motion for a *square* foundation with an embedment a in a half-space subjected to P waves with an incidence $\gamma=30^\circ$.

REFERENCES

- Aki, K. y P.G. Richards (1980), *Quantitative Seismology*, W.H. Freeman, San Francisco.
- Dobry, R. and G. Gazetas (1986). Dynamic response of arbitrarily shaped foundations. *J. Geotech. Engnr. ASCE* 2, **112**, 109-135.
- Kausel, E., R.V. Whitman, J.P. Morray and F. Elsabee (1978). The spring method for embedded foundations, *Nuclear Engineering and Design*, **48**, 377-392.
- Lee, V.W. (1979). Investigation of three-dimensional soil-structure interaction, *University of Southern California*, Dept. of Civil Eng., Rept No CE79-11.
- Sánchez-Sesma, F.J. and F. Luzón (1995). Seismic response of three-dimensional alluvial valleys for incident P , S and Rayleigh waves. *Bull. Seism. Soc. Am.*, **85**, 269-284.
- Sánchez-Sesma, F.J. and M. Campillo (1991). Diffraction of P , SV and Rayleigh waves by topographical features: a boundary integral formulation. *Bull. Seism. Soc. Am.*, **81**, 2234-2253.
- Suarez M. and F.J. Sánchez-Sesma (1995). Dynamic soil-structure interaction for non-axisymmetrical foundations. *Soil Dyn. Earthq. Engnr. VIII*, A.S. Cakmak and C.A. Brebbia (Eds), 485-492.